Evaluation of the Failure Probability of a 2D RC Frame Subjected to Column Loss

Evaluation of the Failure Probability of a 2D RC Frame Subjected to Column Loss

P. Castaldo[1] and E. Miceli[2,*]

[1]*Department of Structural, Geotechnical and Building Engineering (DISEG), Politecnico di Torino, Turin, Italy*

[2]*Department of Structural, Geotechnical and Building Engineering (DISEG), Politecnico di Torino, Turin, Italy*

Abstract: This study regards the evaluation of the failure probability of a symmetrical 2D reinforced concrete frame composed of 4 spans and 5 floors, in case of an accidental event which causes the central base column loss. The frame is an internal one of a typical building designed in a highly seismic area, characterised by a high ductility class. The frame is modelled in the non-linear finite elements software Atena 2D, accounting for both geometrical and material non-linearities. The uncertainties relevant to the problem are included by sampling both material and action variables, adopting the Latin Hypercube Sampling technique. To compute the failure probability associated to the accidental scenario, two sets of analyses are considered: the first set to compute the capacity of the structure against the column removal by means of displacement-controlled pushdown analysis; the second set to evaluate the demand in terms of external loads, properly combined within the accidental combination according to the codes. The external load is then amplified in order to include the dynamic effects characterising a scenario of a structural member loss. Finally, the probability of the demand exceeding the capacity is evaluated.

Keywords: Low-probability high-consequence events, NLFE pushdown analysis, Probabilistic analysis, Reinforced concrete frame, Column loss, Static approach.

1. INTRODUCTION

Nowadays structural engineering community is facing the need of developing adequate tools to deal with extreme events that, in the past, were not considered in performing structural analysis. Those events, which are also defined as low-probability high-consequence (LPHC) events, are capable of determining critical conditions for structures and infrastructures, implying tremendous losses of human, environmental and economic nature. Risk analysis should become part of the strategies for collapse prevention against those events, in order to investigate both socially acceptable and technically feasible solutions [1].

To evaluate the level of safety associated to LPHC events, quantitative risk analysis in probabilistic terms is considered to be a reliable methodology, since it allows to deal with the uncertainties that affect the engineering problems [2]. For example, in [3] a sensitivity analysis to evaluate the bearing capacity of different reinforced concrete (RC) structural members against the removal of a central support is performed. The uncertainties in the collapse demands and resisting capacities of the connections in moment-resisting steel frames is evaluated in [4]. The probability of exceedance of different damage states given a column loss scenario for RC buildings are evaluated in [5], by performing fragility analyses. Global variance-based sensitivity analysis is elaborated in [6], in order to study the major sources of uncertainties in the response of RC structures subjected to sudden column removal. A reliability-based index of structural collapse in case of extreme events is computed in [7], for 2D linear elastic truss systems with random strengths and loads. A probabilistic risk assessment is used in [8] to evaluate the risk of terroristic attacks as different blast scenarios involving built infrastructures, studying their effects on structural and load-capacity systems.

Currently, the traditional design of RC structures does not account for the strength reserves when large deformation and non-linearities are involved due to the occurrence of extreme events which cause the loss of a bearing structural element.

Hence, this paper deals with the evaluation of the probability of failure of a 2D RC frame, designed in seismic area, in case of an event of accidental nature which causes the loss of the central base column. The cause of this collapse scenario can be of different nature: *e.g.*, gas explosion, fire, foundation failure due to natural event. After having defined the geometrical, mechanical and detailing characteristics, the frame has been modelled in the finite element method (FEM) software Atena 2D. Then, a probabilistic sampling with

*Address correspondence to this author at the Department of Structural, Geotechnical and Building Engineering (DISEG), Politecnico di Torino, Turin, Italy; Tel: +39 0110905305;
E-mail: elena.miceli@polito.it

E-ISSN: 2409-9848/23

the Latin Hypercube Sampling method has been performed in order to compute the probability of failure associated to the accidental event. In particular, the number of samples has been assumed equal to 100 and both material (*i.e*., concrete and steel) and actions (*i.e*., permanent and variable loads) variables are sampled. Thus, two sets of analyses are considered: the first set of 100 non-linear displacement controlled pushdown analyses to compute the capacity of the structure against the removal of the central base column; the second set of 100 non-linear static analyses to evaluate the external actions, properly combined according to the accidental code combination, evaluated in the point of column removal. Finally, the probability of the capacity exceeding the demand (*i.e*., the external action) is computed.

2. DESIGN AND FINITE ELEMENT MODELLING OF THE RC FRAME

This study is based on the analysis of a 2D RC frame composed of 4 spans and 5 storeys. The frame is an internal one of a typical building located in a highly seismic area, *i.e*., L'Aquila (Italy), characterized by a ductility class "A". The frame is regular in elevation and symmetrical and is characterised by 5 meters spans and 3 meters inter-storey height (Figure **1**). The influence width in transverse direction is equal to 5 meters.

The design of the structure follows the prescriptions of NTC2018 [9] and EC8 [10]. In particular, according to the combination of gravity loads, live loads, variable loads (including wind and snow) and seismic actions and considering serviceability limit states (SLSs), ultimate limit state (ULSs) and the capacity-design principles, the following geometrical and mechanical characteristics of the frame have been obtained.

All the beams have cross sections of 40x50 cm^2, while all the columns cross sections are of 60x60 cm^2. As for the materials, C25/30 concrete is used while B450C steel is adopted for the reinforcement. The beams are reinforced with ϕ18 for the longitudinal bars and ϕ8 for the transverse reinforcement. In particular, the dissipative area (*i.e*., close to the beam-column nodes) of the beams are arranged with two legs stirrups having 10 cm steps, and the non-dissipative area with two legs stirrups having 15 cm steps. Furthermore, the columns are arranged with 12ϕ20 for the longitudinal reinforcement and ϕ8 four-legs stirrups with 10 cm steps shear reinforcement, except for the beam-column nodes where ϕ10 four-legs stirrups with 5 cm steps are arranged. All the structural elements have a concrete cover of 3.5 cm. The detailing of the longitudinal and transverse reinforcement for the beam is shown in Figure **2**.

The FEM software ATENA 2D [11] is used to model the 2D RC frame. Specifically, four-node quadrilateral iso-parametric plane stress finite elements are used, with linear polynomial interpolation and 2x2 Gauss points integration scheme. The adopted element thickness (in the transverse out-of-plane direction) is equal to 60 cm for the columns and 40 cm for the beams and the mesh size of the elements is in the range 5-10 cm. The non-linear system of equations is solved by means of a linear approximation hypothesis with the standard Newton-Raphson iterative procedure.

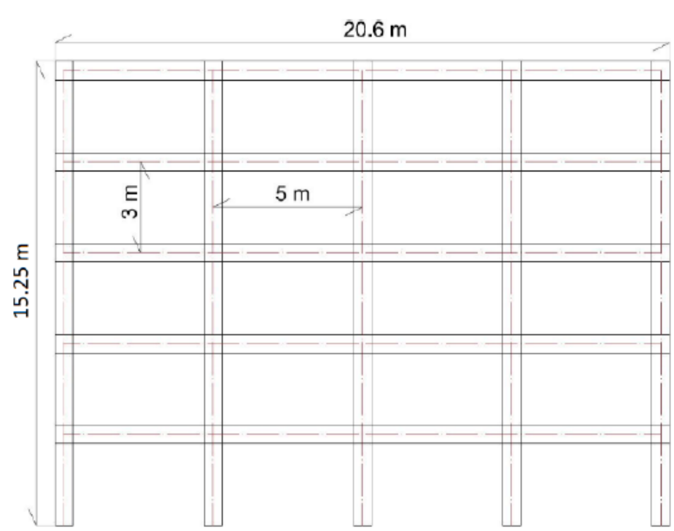

Figure 1: Lateral view of the frame.

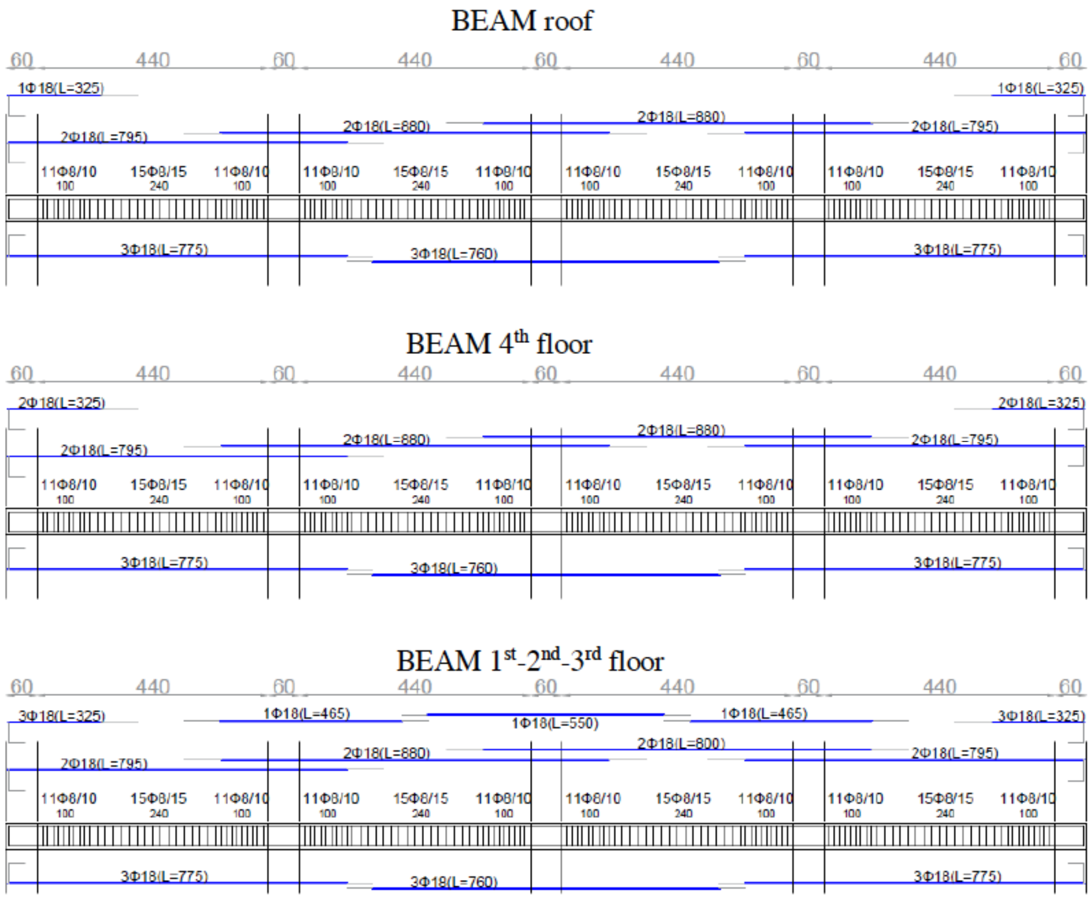

Figure 2: Longitudinal and transverse reinforcement of the beam. The units of measure are in cm.

The concrete is modelled as *SBeta Material.* The behaviour in tension accounts for the tension stiffening effect by means of a linear post-peak branch up to zero strength, while in compression the non-linear response is assumed considering the Saatcioglu and Razvi stress-strain law [12], to include the confinement of concrete. In addition, a reduction of compressive strength and of shear stiffness due to cracks is considered.

The steel is modelled by a bi-linear with hardening constitutive law both in tension and in compression.

Both longitudinal and shear reinforcement is modelled by discrete elements. Geometrical non-linearities are included and perfect bond between concrete and steel is accounted for.

In Figure **3** the geometrical characteristics of the frame as modelled in the FEM software are shown, including the FE nodes, the macro elements and the longitudinal and shear reinforcement configuration. The geometrical scheme adopted provides a subdivision of beams, columns and beam-column nodes, separating for each of them the confined and the unconfined parts as well as the dissipative and the non-dissipative areas of the beams. Finally, fixed constraints are applied to the lines constituting the bases of the columns.

3. PROBABILISTIC ANALYSIS

The rebars detailing of the 2D RC frame is modified before the probabilistic analysis. Indeed, the continuity of the longitudinal rebars at each floor is adopted as useful recommendation suggested in [13-15].

The probabilistic analysis of this work is based on two sets of analyses:

- a set of 100 displacement-controlled push-down non-linear FEM analyses to obtain the capacity curves. From these analyses, the maximum internal reaction given by the structure at the point of the column removal is assessed. This maximum value is herein identified as P_{max}.
- a set of 100 non-linear FEM analyses where the design actions (permanent structural and non-

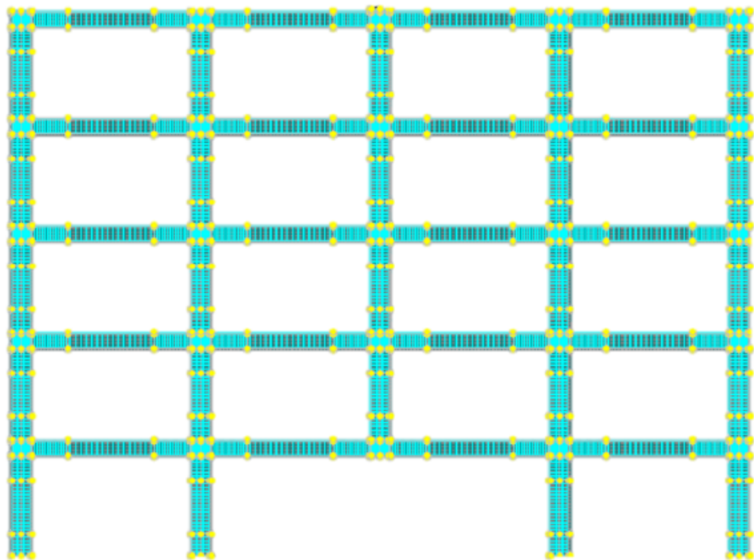

Figure 3: Representation of the 2D FEM model.

structural loads and variable loads) are applied, properly combined adopting the accidental combination according to the current codes [16]. From these analyses, the external action, computed as the reaction to the external loads at the point of column removal, is evaluated. This external action is herein indicated as P_{ext} .

Then, the two values have to be compared according to the static approach prescribed in [17, 18]. In detail, the external load should be amplified by means of a dynamic amplification factor (DAF) that ranges in between 1.0-2.0, to account for the dynamicity associated to the sudden loss of a structural member. In the following, a DAF of 1.2 is adopted in line with other studies [19, 20], since the maximum value of 2.0 is considered too conservative. In this work, the comparison is elaborated within a probabilistic analysis in order to evaluate the safety associated to the structure in case of accidental column removal.

3.1. Probabilistic Sampling

A probabilistic sampling is conducted on 10 basic variables X_i. Specifically, it is accounted for the aleatory nature of both the actions and material properties. For the former, the random variables are: self weight of the structural elements ρ (*i.e.*, specific weight of reinforced concrete), permanent structural load G_1; permanent non-structural load G_2; floor live loads Q_f; roofing live loads Q_r . For the latter, the random variables are: reinforcing steel elastic modulus E_s; reinforcing steel yielding strength f_y; reinforcing steel ultimate strength f_u; reinforcing steel ultimate strain ε_{su}; concrete compressive strength f_c. It is worth noting that each numerical model is subjected to epistemic uncertainty which in this work are not included [21].

In this work, a Latin Hypercube Sampling technique has been adopted, where each variable is sampled from its probabilistic distribution and, subsequently, it is randomly combined with the others. Then, 100 different structural models are obtained by changing 100 times the sampled basic variables. In particular, a Normal distribution is assumed for the permanent loads, a Gumbel distribution for the variable loads [22] while both Lognormal and Normal distributions are considered for the material properties [23].

The coefficients of variation of the random variables have been included in line with [23, 24]. As concerns the mean values, the design values coming from the computation of the influence area have been assumed for the loads, while the mean properties according to the current codes are considered for the materials. Table **1** represents a summary of the statistical parameters regarding the distributions of the different random variables.

In addition, the correlation among variables is included [16]. In particular, the yielding strength f_y and the ultimate strength f_u are correlated adopting a coefficient of 0.75, the yielding strength f_y and the ultimate strain ε_{su} have a correlation coefficient of -0.45 and, finally, the ultimate strength f_u and the ultimate

Table 1: Statistical Parameters and Probabilistic Distribution of the Random Variables

	Distribution	Mean Value	Coefficient of Variation [-]
ρ	Normal	25 [kN/m^3]	0.05
G_1	Normal	16 [kN/m]	0.05
G_2	Normal	13 [kN/m]	0.05
Q_f	Gumbel	6.5 [kN/m]	0.20
Q_r	Gumbel	1.6 [kN/m]	0.20
E_S	Lognormal	210000 [N/mm^2]	0.03
f_y	Lognormal	488.57 [N/mm^2]	0.05
f_u	Lognormal	561.86 [N/mm^2]	0.05
ε_{su}	Lognormal	0.14 [-]	0.09
f_C	Lognormal	31.86 [N/mm^2]	0.15

strain ε_{su} are correlated by means of a coefficient of -0.60. The correlation coefficients are shown in Table **2**.

Table 2: Correlation Coefficients Among Steel Basic Variables

	f_y	f_u	ε_u
f_u	1	0.75	-0.45
f_u	0.75	1	-0.60
ε_u	-0.45	-0.60	1

3.2. Pushdown Analyses and Evaluation of the Capacity

In this section, the first set of analyses is described. In particular, 100 non-linear FEM pushdown analyses have been computed by varying materials characteristics. To evaluate the capacity of a structure against the loss of a supporting element, displacement-controlled pushdown analyses are effective since they allow the computation of the corresponding displacement-force curves [25, 26]. Hence, the structure is modelled without the accidentally lost column (*i.e*., the central base column) and an increasing vertical displacement is applied at the top of the lost structural element. For each step, the reaction at the point of application of the imposed displacement is computed. In this way, the load-displacement or capacity or pushdown curves are computed for each one of the 100 aleatory combinations. In this phase, no other external loads are applied.

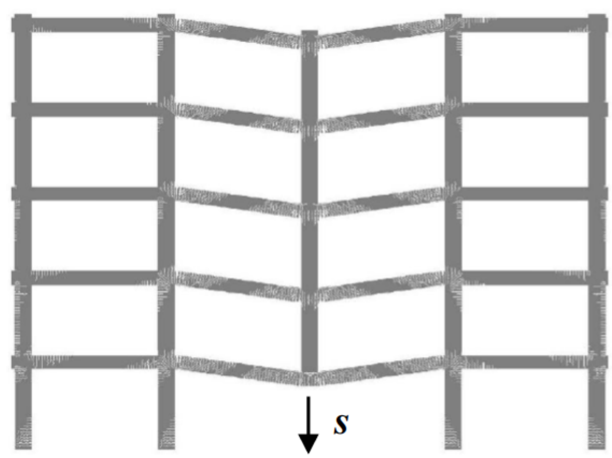

Figure 4: Scheme of the first set of non-linear static analyses: pushdown analysis.

In the following, the results in terms of capacity curve are shown for the 100 non-linear FEM analyses (Figure **5**). For all the capacity curves, three stages can be recognised:

- the first stage (flexural stage), which lasts up to the first peak (hereafter indicated as $P_{flex,peak}$), is characterised by a response that remains in the linear elastic field until non-linear material behaviour becomes dominant. In the last phase of this stage the compressive axial effect governed by concrete properties and due to cracks openings guarantees a certain resistance reservoir which is capable to bear the load until the maximum flexural behaviour is reached; the first stage peak represents the condition in which the maximum flexural resistance is reached.

- the second stage (softening stage) occurs after the first peak, where plastic hinges form and the compressive axial effects decrease, implying a drop in resistance followed by a constant reaction. This stage is defined as softening stage.
- the third and last stage (catenary stage), implies a recovery in resistance. This behaviour is due to the tensile axial actions to which the beams are subjected thanks to the presence of the longitudinal reinforcement which behaves as a tie. This plateaux stage continues until the ultimate resistance is reached.

In Figure **5** results in terms of capacity curves are shown. In particular, in Figure **5**(**b**) the loads have been normalized with respect to the value of the first peak $P_{flex,peak}$, while the displacements have been normalized with respect to the value of the imposed displacement corresponding to that peak.

In the majority of the cases the maximum load P_{max} (*i.e.*, black stars of Figure **5**) is reached in correspondence of the peak of the first stage $P_{flex,peak}$, and during the softening stage the eventual recovery in resistance does not lead to an overcome of the first resistance peak. However, there are certain cases where the ultimate resistance before failure overcomes the initial peak. These cases are registered when the sampled ultimate strains of the steel reinforcement are quite large with respect to the mean value (*i.e.*, 0.14), since the catenary behaviour is favoured by a more ductile reinforcement response. The maximum load P_{max}, that is the maximum value of the capacity curve obtained from each of the 100 simulations, oscillates between a minimum of 1198 kN and a maximum of 1554 kN. In general, the minimum of these loads is obtained when there is a combination of poor characteristics of both concrete and steel material properties, while the opposite occurs for the larger values. The P_{max} parameter has a mean value of 1349 kN and a standard deviation of 64.42 kN.

A statistical inference analysis has followed to evaluate which type of distribution best fits the data obtained in terms of P_{max}. In particular, the Normal, Lognormal and Gumbel distributions have been tested by applying both the Chi-Square and the Anderson Darling tests with significance level of 5%. The

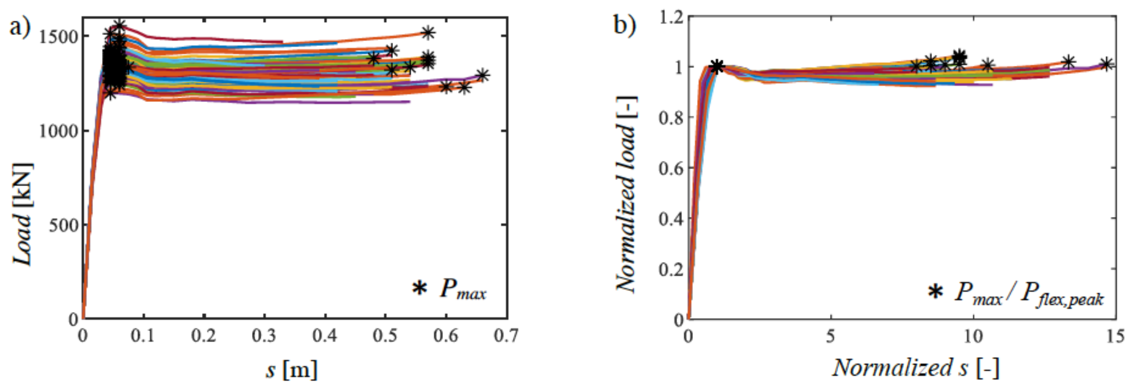

Figure 5: Results of the 100 non-linear pushdown analyses: **a**) load-displacement capacity curve; **b**) normalized load-displacement capacity curve.

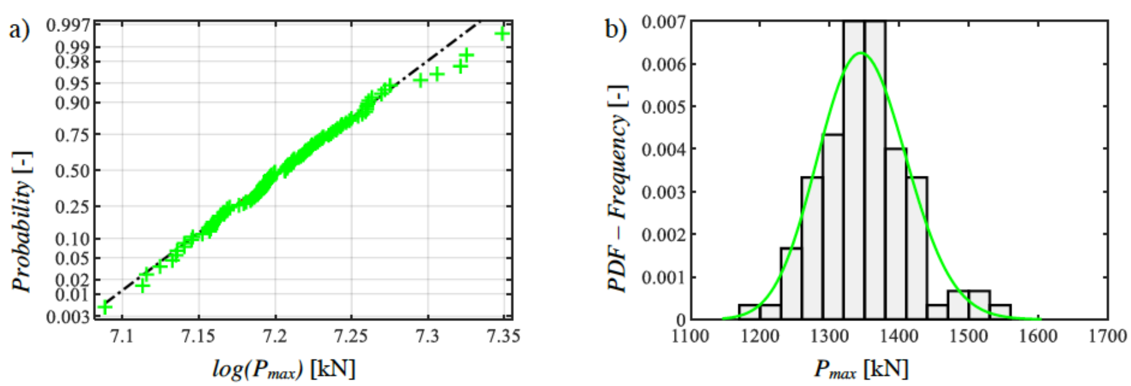

Figure 6: Probabilistic evaluation of P_{max}: **a**) probability plot; **b**) histogram and probability density function.

lognormal distribution has been selected as the proper probabilistic distribution since it has passed the goodness of fit test with the largest p-value of 0.67 among the three distributions. In Figure **6** the results of the statistical inference are shown. In particular, the probability plot (Figure **6** (**a**)) of the logarithm of the data shows that data are aligned on a straight line confirming the goodness of the tests. In Figure **6**(**b**) the Lognormal Probability Distribution Function (PDF) is plotted together with the histogram of the data.

3.3. Evaluation of the Demand

The second step of this study consists in computing the external load, by assuming that it coincides with the reaction due to the external loads (combined according to the accidental combination [9, 16]) at the point where the column is accidentally lost. These reactions can be calculated considering the actions sampled through the *LHS* procedure.

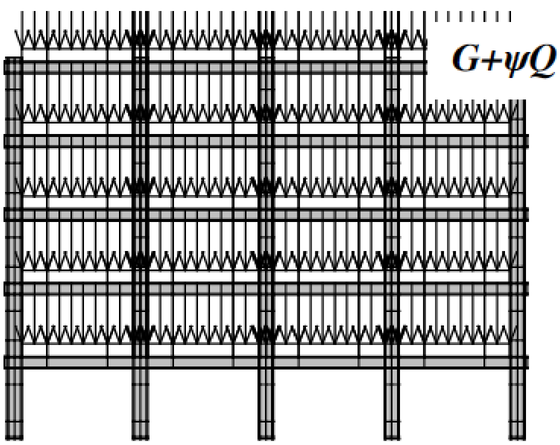

Figure 7: Scheme of the second set of non-linear static analyses.

The value of the external load P_{ext} ranges from a maximum value of 1186 kN, to a minimum value of 976 kN, the mean is equal to 1061 kN, while the standard deviation equals 41.27 kN. Of course, the maximum value of the external load is obtained when there is a combination of large values of actions from the LHS sampling.

Also for the external load, a statistical inference analysis has been applied. In particular, the Normal, Lognormal and Gumbel distributions have been tested by applying both the Chi-Square and the Anderson Darling tests with significance level of 5%. The lognormal distribution has been selected as the proper probabilistic distribution since it has passed the goodness of fit test with the largest p-value of 0.79 among the three distribution. In Figure **8** the results of the statistical inference are shown. In detail, the probability plot (Figure **8**(**a**)) of the logarithm of the data shows that data are aligned on a straight line confirming the goodness of the tests. In Figure **8**(**b**) the Lognormal Probability Distribution Function (PDF) is plotted together with the histogram of the data.

According to the static approach [17, 18], the external load is amplified through a dynamic coefficient equal to 1.2, in order to account for moderate dynamic effects. In the following, the amplified external load is identified as $P_{ext,ampl}$.

3.4. Computation of the Probability of Failure Associated to the Accidental Scenario

To formulate the structural reliability problem, the uncertain variables have been modelled as n=10 basic random variables. The space governed by these input variables is divided by the limit state function into two regions: a safe and an unsafe region. The limit state function *Z* identifies the condition beyond which the structural system does not satisfy one of its performance requirements [27, 28]. The safe region is the space where Z is positive or equal to zero, while

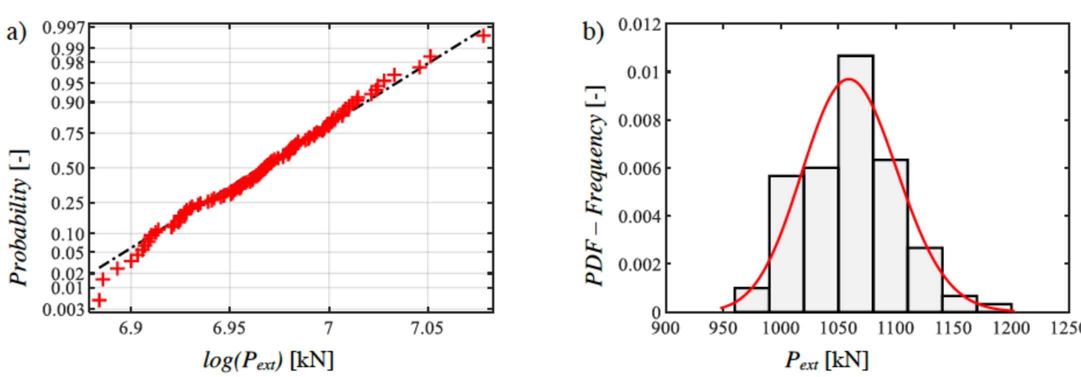

Figure 8: Probabilistic evaluation of P_{ext}: **a**) probability plot; **b**) histogram and probability density function.

the failure region elsewhere. Thus, the probability of failure P_f is the probability that the limit state function is negative. An alternative measure of the structural reliability can be expressed by the reliability index β, formulated as the negative value of the inverse of the standard normal variable evaluated in correspondence of the probability of failure P_f [29, 30].

In this work, the limit state function can be formulated as the difference between the capacity R and the demand A. In our problem formulation, the capacity is intended as the internal reaction given by the structure in the event of the accidental column removal (*i.e.*, P_{max}), while the demand is the reaction due to the external loads at the same point, amplified by the dynamic amplification coefficient (*i.e.*, $P_{ext,ampl}$). Thus, the limit state function can be written as:

$$Z = R - A = P_{max} - P_{ext,ampl} \tag{1}$$

From this formulation, it follows that the probability of failure associated with the accidental scenario can be computed as:

$$P_f = P(Z<0) = \Phi\left(\frac{0-\mu_Z}{\sigma_Z}\right) \tag{2}$$

where Φ is the cumulative density function of the standard distribution, μ_Z and σ_Z are, respectively, the mean and the standard deviation of the limit state function computed as:

$$\mu_Z = \mu_{Pmax} - \mu_{Pext,ampl}\ ; \quad \sigma_Z = \sqrt{\sigma^2_{Pmax} + \sigma^2_{Pext,ampl}} \tag{3}$$

assuming that the two variables P_{max} and $P_{ext,ampl}$ are independent and are described by corresponding Lognormal distributions.

By applying the formula in (2), the probability of failure associated with the loss of the central base column of the frame is equal to $1.75\cdot10^{-1}$. This large value of failure probability can be graphically understood by looking at the probability density functions of the demand and the capacity in Figure **9**(**a**) and the graphical representation of the limit state function in Figure **9**(**b**). Indeed, the distribution of the demand (in terms of amplified external load) is close to the distribution of the capacity, leading to a large value of the associated failure probability. This results should be compared with a *de minimis* risk (*i.e.*, an acceptable risk level), established of the order between 10^{-2}/year and 10^{-1}/year [31], if identified in terms of conditional probability of collapse (*i.e.*, given that the loss of the bearing column has occurred). It is worth to note that a strong influence is due to the dynamic effects involved in such a problem [32]. At the same time, this probability of failure should be analyzed in a wider context of risk management [31]. Furthermore, the 2D RC frame is not designed considering particular suggestions to improve the mechanical response when a column is removed.

4. CONCLUSIONS

In this work it is evaluated the probability of failure of a symmetrical 2D reinforced concrete frame composed of 4 spans and 5 floors, in case of an extreme event which causes the central base column loss. The structural system is an internal frame of a typical building designed in a highly seismic area in Italy, considering a high ductility class. After having performed the design of the structure considering ultimate limit state, serviceability limit state and capacity design verifications, the frame is modelled in the FEM software Atena 2D, where it is accounted for geometrical and material non-linearities. With the

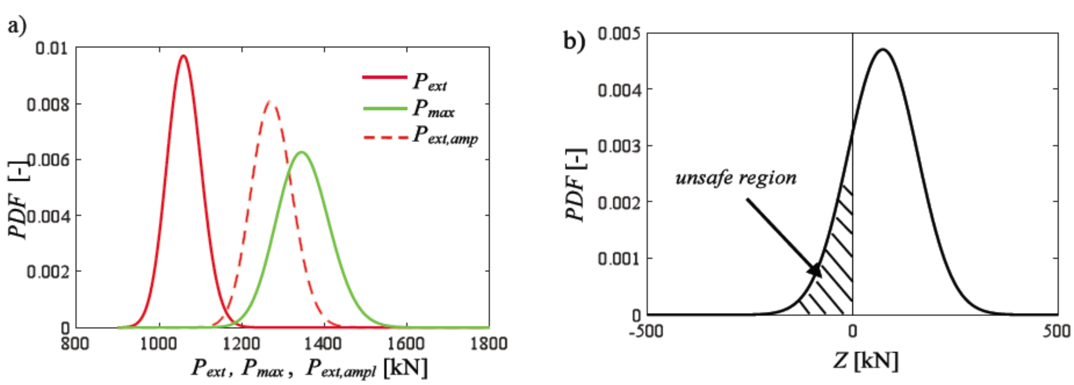

Figure 9: Computation of the failure probability: **a**) comparison between the probability density functions of both the capacity (*i.e.*, P_{max}) and demand (*i.e.*, P_{ext} and $P_{ext,ampl}$); **b**) limit state function and unsafe region.

scope of performing a full-probabilistic analysis, the Latin Hypercube Sampling technique is adopted. In particular, material (*i.e*., yielding strength, ultimate strength, ultimate strain and elastic modulus of reinforcing steel and concrete compressive strength) and actions (*i.e*., self weight, permanent structural and non structural loads and live loads) variables are randomly sampled, considering a number of sampling equal to 100. Then, two sets of analyses are considered: the first set of 100 non-linear FEM pushdown analyses to evaluate the capacity of the structure against the column removal and the second set of static non-linear analyses to calculate the demand in terms of external action, combined within the accidental combination prescribed in current codes, at the point of the column removal. By performing a statistical inference, both capacity and demand has resulted to be lognormally distributed with mean 1349 kN and 1061 kN, respectively, and standard deviation of 64.42 kN and 41.27 kN, respectively. According to the static approach, the demand in terms of external load is amplified by a dynamic coefficient equal to 1.2 in order to include moderate dynamic effects. Finally, the probability of failure associated to the probability of the demand exceeding the capacity is computed and equals $1.75 \cdot 10^{-1}$. Future works should consider the fact that the result is strongly affected by the dynamic amplification factor used to amplify the demand as well as suggestions to improve the mechanical response when a column is removed.

CONFLICT OF INTEREST

No conflict of interest.

AKNOWLEDGEMENTS

This work is part of the collaborative activity developed by the authors within the framework of the Commission 3 – Task Group 3.1: *"Reliability and safety evaluation: full-probabilistic and semi-probabilistic methods for existing structures"* of the International Federation for Structural Concrete (*fib*).

This work is also part of the collaborative activity developed by the authors within the framework of the WP 11 – Task 11.4 – ReLUIS.

This work is also part of the collaborative activity developed by the authors within the framework of the Action Group "Robustness" of the International Federation for Structural Concrete (*fib*).

This work is also part of the collaborative activity developed by the authors within the framework of the "PNRR - VS3 "Earthquakes and Volcanos" - WP3.6".

REFERENCE

[1] Ellingwood BR. Mitigating risk from abnormal loads and progressive collapse. J. Perform. Constr. Facil. 2006; 20(4): 315-323. https://doi.org/10.1061/(ASCE)0887-3828(2006)20:4(315)

[2] JCSS. Probabilistic Model Code, Part 1 - Basis of Design 2000.

[3] Botte W, Droogné D, Caspeele R. Reliability-based resistance of RC element subjected to membrane action and their sensitivity to uncertainties. Eng. Struct. 2021; 238: 112259. https://doi.org/10.1016/j.engstruct.2021.112259

[4] Xu G, Ellingwood B. Probabilistic Robustness Assessment of Pre-Northridge Steel Moment Resisting Frames. J. Struct. Eng. 2011; 137(9): 925-934. https://doi.org/10.1061/(ASCE)ST.1943-541X.0000403

[5] Brunesi E, Nascimbene R, Parisi F, et al. Progressive Collapse Fragility of Reinforced Concrete Framed Structures through Incremental Dynamic Analysis. Eng. Struct. 2015; 104: 65-79. https://doi.org/10.1016/j.engstruct.2015.09.024

[6] Arshian A, Morgenthal G, Narayanan S. Influence of modelling strategies on uncertainty propagation in the alternate path mechanism of reinforced concrete framed structures. Eng. Struct. 2016; 110: 36-47. https://doi.org/10.1016/j.engstruct.2015.11.019

[7] Bhattacharya B. A reliability based measure of structural robustness for coherent systems. Struct. Saf. 2021; 89: 102050. https://doi.org/10.1016/j.strusafe.2020.102050

[8] Stewart M, Netherton M, Rosowsky D. Terrorism Risks and Blast Damage to Built Infrastructure. Nat. Haz. Rev. 2006; 7(3): 114-122. https://doi.org/10.1061/(ASCE)1527-6988(2006)7:3(114)

[9] MIT, Istruzioni per l'applicazione dell'«Aggiornamento delle "Norme tecniche per le costruzioni"» di cui al decreto ministeriale 17 gennaio 2018, 2019.

[10] European Committee for Standardization, Eurocode 8 - Design of Structures for earthquake resistance, 1998.

[11] Cervenka Consulting s.r.o., ATENA 2D v5, Prague, Czech Republic, 2014.

[12] Saatcioglu M, Razvi SR. Strength and ductility of confined concrete. J. Struct. Eng. 1993; 119(10): 3109-3110. https://doi.org/10.1061/(ASCE)0733-9445(1993)119:10(3109)

[13] Department of Communities and Local Government. The building regulations 2010 - structure: approved document A. UK: HM Government; 2010.

[14] ASCE Standard 7-02, Minimum Design Loads for Buildings and Other Structures (ASCE 7-16) (2016), American Society of Civil Engineers, Reston, VA.

[15] Adam J M, Buitrago M, Bertolesi E, et al. Dynamic Performance of a Real-scale Reinforced Concrete Building Test under a Corner-column Failure Scenario. Eng. Struct. 2020; 210: 110414. https://doi.org/10.1016/j.engstruct.2020.110414

[16] European Committee for Standardization, Eurocode 1 - Actions on structures - Part 1-7: General actions - Accidental actions, 1991.

[17] General Services Administration (GSA). Alternative path analysis and design guidelines for progressive collapse resistance. Washington, DC: Office of Chief Architects; 2013.

[18] United States Departement of Defence (DoD), Unified Facilities Criteria (UFC): design of buildings to resist progressive collapse, Washington, D.C., Nov. 2016.

[19] Kaewkulchai G, Williamson EB. Beam element formulation and solution procedure for dynamic progressive collapse analysis. Comput. Struct.2004; 82(7-8): 639-651. https://doi.org/10.1016/j.compstruc.2003.12.001

[20] Pretlove AJ, Ramsden M, Atkins A. Dynamic effects in progressive failure of structures. Int. J. Impact Eng. 1991; 11(4): 539-546. https://doi.org/10.1016/0734-743X(91)90019-C

[21] Gino D, Castaldo P, Giordano L, Mancini G. Model Uncertainty in Non-linear Numerical Analyses of Slender Reinforced Concrete Members. Struct. Concr. 2021; 845-70. https://doi.org/10.1002/suco.202000600

[22] JCSS, Probabilistic Model Code, Part 2 - Load Models., 2001.

[23] JCSS, Probabilistic Model Code, Part 3 - Resistance Models, 2002.

[24] Fib, Model Code for Concrete Structures, 2010.

[25] Khandelwal KS, El-Tawil S. Pushdown resistance as a measure of robustness in progressive collapse analysis, Eng. Struct. 2011; 33(9): 2653-2661. https://doi.org/10.1016/j.engstruct.2011.05.013

[26] Ferraioli M, Avossa AM, Mandara A. Assessment of Progressive Collapse Capacity of Earthquake-Resistant Steel Moment Frames Using Pushdown Analysis. Open Constr. Build. Technol. J. 2014; 8(1): 324-336. https://doi.org/10.2174/1874836801408010324

[27] Fib, Partial factor methods for existing concrete structures. Bulletin no. 80: 2016.

[28] CEN EN 1990 Eurocode. 2002. "Basis of structural design." Brussels.

[29] Implementation of Eurocodes Handbook 2 - Reliability backgrounds. Leonardo Da Vinci Project. Prague, 2005.

[30] ISO 2394: 2015: General principles on reliability for structures. Genéve, 2015.

[31] Paté-Cornell M. (1994). Quantitative safety goals for risk management of industrial facilities. Struct. Saf. 1994; 13(3): 145-157. https://doi.org/10.1016/0167-4730(94)90023-X

[32] Izzuddin BA, Vlassis AG, Elghazouli AY, Nethercot DA. Progressive collapse of multi-storey buildings due to sudden column loss - Part I: Simplified assessment framework. Eng. Struct. 2008; 30(5): 1308-1318. https://doi.org/10.1016/j.engstruct.2007.07.011

Received on 12-12-2022 Accepted on 04-01-2023 Published on 07-01-2023

DOI: https://doi.org/10.31875/2409-9848.2023.10.01